Weak solution of the nonuniform multiconductor transmission lines

Weak Solution of the Nonuniform Multiconductor Transmission Lines

S. Grivet-Talocia
Dip. Elettronica, Politecnico di Torino
Corso Duca degli Abruzzi 24
I-10129, Torino, Italy

F. Canavero
Dip. Elettronica, Politecnico di Torino
Corso Duca degli Abruzzi 24
I-10129, Torino, Italy

Abstract: A time domain technique for the simulation of Nonuniform Multiconductor Transmission Lines (NMTL) with external sources is presented. The technique is based on a weak formulation of the NMTL equations obtained through expansion of the voltage and current vectors, per unit length matrices, and distributed sources into a set of locally supported basis functions. The particular choice of these functions determines the approximation order of the method. Examples are shown for practical interest structures.

INTRODUCTION

This paper presents a new time domain simulation method for the Nonuniform Multiconductor Transmission Lines equations. This topic has been collecting a lot of interest in the recent literature, because many interconnections of practical interest are characterized by cross sections which are not translation-invariant. Examples can be impedance matching networks or cables in complex structures, like automobiles or airplanes. Therefore, it is of crucial importance to model the effects of the nonuniformity of the interconnections both from signal integrity and EMI standpoints.

Several techniques have been presented for the simulation of the NMTLs. These techniques can be subdivided in two main classes, performing simulation in the frequency domain or in the time domain, respectively. The former can obtain closed-form solutions [1] in some cases, but can also be used to analyze more general structures through a piecewise constant discretization of the line [2]. If the transient response is wanted, inverse FFT can be used. However, when signals with complex waveforms are applied to unmatched lines and long transients are generated, the number of points for the evaluation of the FFT can be very large. In fact, as the result of inverse FFT is always a periodic waveform, the period must be chosen long enough for the transients to be extinguished. This is the reason why numerical schemes performing the simulation directly in the time domain have been recently proposed. Among these we can cite the methods based on the scattering representation [5], the method of characteristics [9], and the waveform relaxation analysis [4]. The method presented here is based on a weak formulation of the NMTL equations, which leads to a class of numerical schemes of different approximation order according to the particular choice of some trial and test functions.

MATHEMATICAL FORMULATION

Let us consider the NMTL equations

$$\frac{\partial}{\partial z}\mathbf{V}(z,t) + \mathbf{L}(z)\frac{\partial}{\partial t}\mathbf{I}(z,t) + \mathbf{R}(z)\mathbf{I}(z,t) = \mathbf{V_F}(z,t),$$
$$\frac{\partial}{\partial z}\mathbf{I}(z,t) + \mathbf{C}(z)\frac{\partial}{\partial t}\mathbf{V}(z,t) + \mathbf{G}(z)\mathbf{V}(z,t) = \mathbf{I_F}(z,t),$$

with $\mathbf{V}(z,t)$ and $\mathbf{I}(z,t)$ indicating the voltage and current vectors at location z and time t. The line is assumed to have $P+1$ conductors, and the per-unit-length parameters $\mathbf{L}(z)$, $\mathbf{C}(z)$, $\mathbf{R}(z)$, and $\mathbf{G}(z)$ are $P \times P$ matrices whose entries are arbitrary functions of the space variable z. Without loss of generality we will consider the length of the line to be normalized, i.e., $z \in [0,1]$. The distributed sources $\mathbf{V_F}$ and $\mathbf{I_F}$ are due to external field excitation and must be known at any z and t. For simplicity, the line is supposed here to be terminated by Thévénin loads,

$$\mathbf{V}(0,t) = \mathbf{V_S}(t) - \mathbf{R_S}\mathbf{I}(0,t), \quad (1)$$
$$\mathbf{V}(1,t) = \mathbf{V_L}(t) + \mathbf{R_L}\mathbf{I}(1,t). \quad (2)$$

However, any other type of linear and resistive terminations can be used with the following formulation.

The approximate voltages and currents along the line are sought for in terms of expansion coefficients into a set of trial functions $\{\varphi_n : n = 1, \ldots, N_\varphi\}$,

$$\mathbf{V}(z,t) = \sum_{n=1}^{N_\varphi} \varphi_n(z)\mathbf{V}_n(t), \quad (3)$$

$$\mathbf{I}(z,t) = \sum_{n=1}^{N_\varphi} \varphi_n(z)\mathbf{I}_n(t). \quad (4)$$

The external sources are also projected onto the same ap-

0-7803-5015-4/98/$10.00 © 1998 IEEE

proximation space through the expansion

$$\mathbf{V_F}(z,t) = \sum_{n=1}^{N_\varphi} \varphi_n(z)\mathbf{V_F}_n(t), \quad (5)$$

$$\mathbf{I_F}(z,t) = \sum_{n=1}^{N_\varphi} \varphi_n(z)\mathbf{I_F}_n(t). \quad (6)$$

A similar expansion can be used, with possibly different basis functions $\{\phi_k : k = 1,\ldots,N_\phi\}$, for the entries in the per unit length matrices

$$\mathbf{L}(z) = \sum_{k=1}^{N_\phi} \phi_k(z)\mathbf{L}_k,$$

and similarly for $\mathbf{C}(z)$, $\mathbf{R}(z)$, and $\mathbf{G}(z)$. Projecting now the NMTL equations onto a third set of functions $\{\eta_m : m = 1,\ldots,N_\varphi\}$, we get a set of ODE's representing the spatial discretization of the original NMTL equations,

$$\sum_{n=1}^{N_\varphi} \mathbf{\Lambda}_{mn}\mathbf{V}_n(t) + \sum_{n=1}^{N_\varphi} \widehat{\mathbf{L}}_{mn}\frac{d}{dt}\mathbf{I}_n(t) + \sum_{n=1}^{N_\varphi} \widehat{\mathbf{R}}_{mn}\mathbf{I}_n(t) = \sum_{n=1}^{N_\varphi} \mathbf{E}_{mn}\mathbf{V_F}_n(t), \quad (7)$$

$$\sum_{n=1}^{N_\varphi} \mathbf{\Lambda}_{mn}\mathbf{I}_n(t) + \sum_{n=1}^{N_\varphi} \widehat{\mathbf{C}}_{mn}\frac{d}{dt}\mathbf{V}_n(t) + \sum_{n=1}^{N_\varphi} \widehat{\mathbf{G}}_{mn}\mathbf{V}_n(t) = \sum_{n=1}^{N_\varphi} \mathbf{E}_{mn}\mathbf{I_F}_n(t), \quad (8)$$

with

$$\mathbf{\Lambda}_{mn} = \langle \frac{d}{dz}\varphi_n, \eta_m\rangle\, \mathcal{I}_P,$$
$$\mathbf{E}_{mn} = \langle \varphi_n, \eta_m\rangle \mathcal{I}_P,$$
$$\widehat{\mathbf{L}}_{mn} = \sum_{k=1}^{N_\phi} \mathbf{L}_k B^{(k)}_{mn},$$

where $\mathcal{I}_P$ is the $P \times P$ identity matrix, and

$$B^{(k)}_{mn} = \langle \varphi_n\ \phi_k, \eta_m\rangle. \quad (9)$$

Similar expressions hold for $\widehat{\mathbf{C}}_{mn}$, $\widehat{\mathbf{R}}_{mn}$, and $\widehat{\mathbf{G}}_{mn}$.

We consider now the inclusion of the loads (1) and (2). It is convenient to choose the trial and test functions such that only one is nonzero at the boundaries, i.e.,

$$\begin{aligned} \varphi_n(0) &= 0, \quad \forall n = 2,\ldots,N_\varphi, \\ \varphi_n(1) &= 0, \quad \forall n = 1,\ldots,N_\varphi - 1, \\ \eta_m(0) &= 0, \quad \forall m = 2,\ldots,N_\varphi, \\ \eta_m(1) &= 0, \quad \forall m = 1,\ldots,N_\varphi - 1. \end{aligned} \quad (10)$$

This is not a real restriction because whatever be the initial choice of basis functions, a change of basis can always be performed to obtain only one nonzero function at both edges. The two edge trial functions will also be normalized so that

$$\varphi_1(0) = \varphi_{N_\varphi}(1) = 1.$$

Substituting now the expansions (3) and (4) into the load equations (1) and (2) and using the conditions (10), we get

$$\mathbf{V}_1(t) = \mathbf{V_S}(t) - \mathbf{R_S}\mathbf{I}_1(t) \quad (11)$$
$$\mathbf{V}_{N_\varphi}(t) = \mathbf{V_L}(t) + \mathbf{R_L}\mathbf{I}_{N_\varphi}(t) \quad (12)$$

These expressions for the loads can be used to eliminate the two unknowns $\mathbf{V}_1(t)$ and $\mathbf{V}_{N_\varphi}(t)$ from the system (7)-(8). It should be noted, however, that the number of scalar unknowns in the system is $2N_\varphi P$, which matches the number of scalar equations. If we eliminate the voltages at the two edges, i.e., $2P$ scalar unknowns, also $2P$ equations must be suppressed in order to keep the balance even. These equations are obviously the ones involving the projection onto the border test functions η_1 and η_{N_φ}. As a result, the system of ODE's to be solved reads

$$\begin{aligned} \mathbf{\Psi}\frac{d}{dt}\mathbf{x}(t) + \mathbf{\Phi}\,\mathbf{x}(t) = \\ \mathbf{\Gamma_S}\mathbf{V_S}(t) + \mathbf{\Gamma_L}\mathbf{V_L}(t) + \\ \mathbf{\Gamma_{SD}}\frac{d}{dt}\mathbf{V_S}(t) + \mathbf{\Gamma_{LD}}\frac{d}{dt}\mathbf{V_L}(t) + \\ \mathbf{\Omega_V}\hat{\mathbf{V}}_\mathbf{F}(t) + \mathbf{\Omega_I}\hat{\mathbf{I}}_\mathbf{F}(t) \end{aligned} \quad (13)$$

where $\mathbf{\Psi}$ is nonsingular if the trial and test functions are linearly independent. The array $\mathbf{x}$ collects the expansion coefficients of voltage and current along the line, while the arrays $\hat{\mathbf{V}}_\mathbf{F}$, $\hat{\mathbf{I}}_\mathbf{F}$ collect the time-varying expansion coefficients of the distributed sources.

The system (13) can be solved with a suitable integration method. We used here a a $5^{\text{th}} - 6^{\text{th}}$ order explicit Runge-Kutta scheme [6]. If the trial and test functions have a local support, the system matrices $\mathbf{\Psi}$ and $\mathbf{\Phi}$ have a banded structure with few nonvanishing codiagonals. Therefore, the computation of the product $\mathbf{\Psi}^{-1}\mathbf{\Phi}\mathbf{x}$ can be performed in $O(N_\varphi)$ operations. The same applies to the external forcing terms $\mathbf{\Omega_V}$, $\mathbf{\Omega_I}$. It should be noted that the forcing terms in the system (13) include also the time derivatives of the source vectors $\mathbf{V_S}(t)$ and $\mathbf{V_L}(t)$. Therefore, singular waveforms like delta functions or step functions cannot be handled by this method.

EXAMPLES

The numerical scheme was applied to several examples and validated through comparison with a reference solution, obtained by applying inverse FFT to the frequency domain solution. The weak solution for the following examples was determined with piecewise polynomial (B-splines) basis functions for the three sets φ_n, ϕ_k, and η_m. With these basis functions the approximation error is expected to decrease as N_φ^{-L}, where $L-1$ is the local polynomial order of the basis functions.

Scalar exponential line

We chose the scalar exponential line as a test case for our numerical scheme because the analytical solution in the frequency domain is well known and understood [3].

Let us consider a scalar nonuniform line ($P = 1$) of unitary length characterized by

$$L(z) = L^0 e^{\delta z}, \qquad R(z) = 0,$$
$$C(z) = C^0 e^{-\delta z}, \qquad G(z) = 0,$$

where the parameter δ controls the rate of taper and L^0, C^0 are the nominal per unit length inductance and capacitance at the edge $z = 0$. The nominal characteristic impedance of the line is therefore

$$Z(z) = \sqrt{\frac{L(z)}{C(z)}} = Z_0 e^{\delta z},$$

where Z_0 is the nominal characteristic impedance at the edge $z = 0$. As the impedance level increases at rate δ with z, it can be shown that the positive voltage wave increases in magnitude and the corresponding current wave decreases at rate $\delta/2$. The converse holds for negative voltage and current waves.

The parameters of the line that will be investigated here are normalized. More precisely,

$$L^0 = 1\text{H/m}, \qquad C^0 = 1\text{F/m}, \qquad \delta = \log 4.$$

This corresponds to a 1:4 impedance stepping line. The waveform of the voltage source is set here to a gaussian pulse,

$$v_s(t) = V_0 \exp\left\{-\frac{(t - T_s)^2}{2\Delta_s^2}\right\}, \tag{14}$$

with amplitude $V_0 = 1\text{V}$, center $T_s = 2$ s, and semi-width $\Delta_s = 0.2$ s. The line is matched at both ends.

A reference solution in the time domain is obtained from the frequency domain analytical solution through inverse FFT. The total simulation time is set here to $T_{\max} = 8$ s, which means that the input signal is considered as a periodic pulse train with period $T_{\max}$. As the one-way delay is $T = 1$ s, there are no interactions between two adjacent pulses, because the transient associated to one pulse due to the nonuniformity of the line is already extinguished when the next pulse comes through. Of course, this holds only when at least one of the two line ends is matched.

The voltage at the two terminations obtained with the weak formulation by using piecewise linear functions is plotted and compared to the reference solution in Figure 1. The number of basis functions in these simulations is $N_\varphi = 65$. The figures show clearly that the weak solution (thin continuous line) is undistinguishable from the reference solution (thick dashed line).

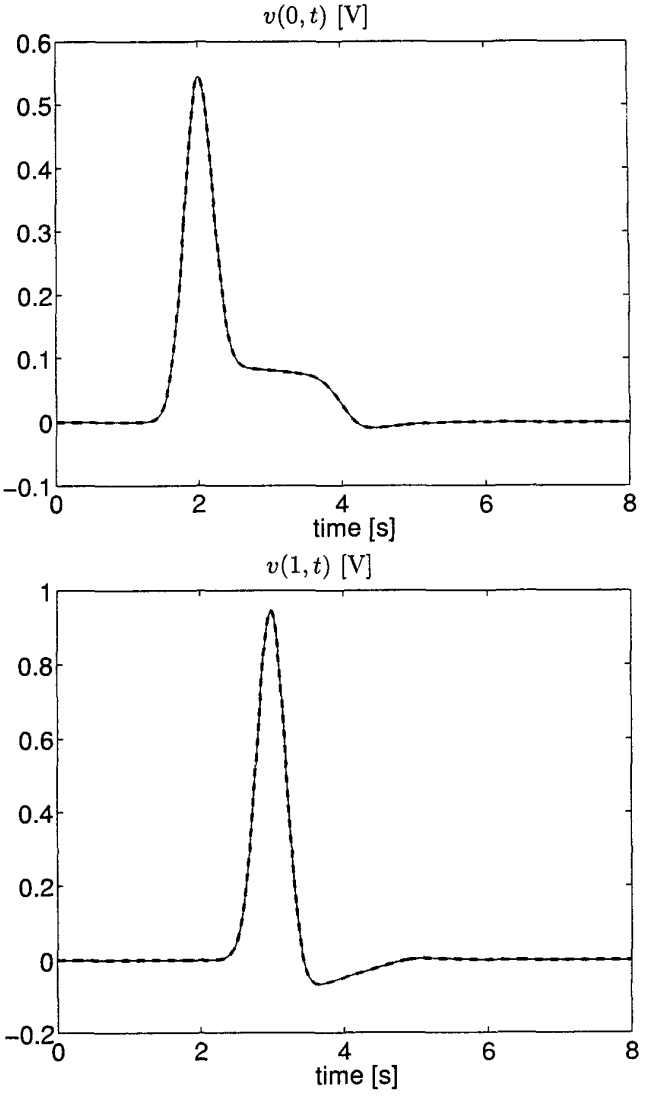

Figure 1: Voltage at the left (top panel) and right (bottom panel) terminations of the matched 1:4 exponential line.

The convergence properties of the method as the dimension N_φ of the approximation spaces increases is now investigated. The approximation error on voltage and current is computed for each N_φ according to

$$E_v(N_\varphi) = \max_t \max_z |v_{N_\varphi}(z,t) - v_{\text{ref}}(z,t)|,$$
$$E_i(N_\varphi) = \max_t \max_z |i_{N_\varphi}(z,t) - i_{\text{ref}}(z,t)|,$$

where $v_{\text{ref}}(z,t)$, $i_{\text{ref}}(z,t)$ represent the reference voltage and current while $v_{N_\varphi}(z,t)$, $i_{N_\varphi}(z,t)$ are the voltage and current obtained with our method. The voltage approximation errors are reported in Figure 2 as functions of N_φ. The parameter L controls the approximation order of the

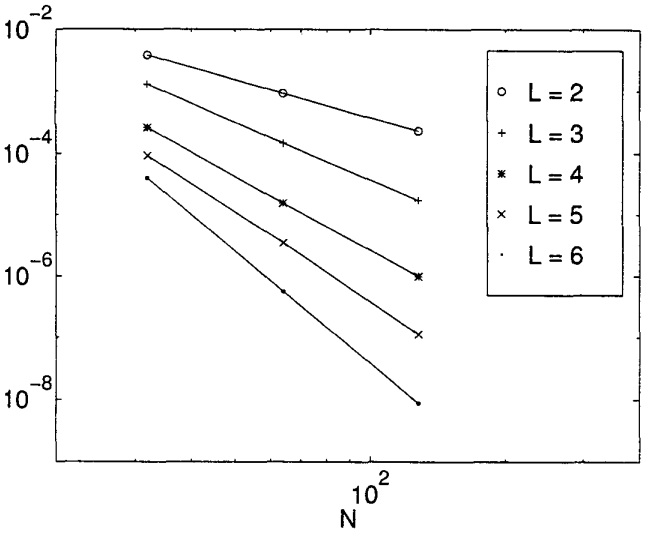

Figure 2: Matched 1:4 exponential line with gaussian excitation. Maximum absolute error on voltage as a function of N_φ and of the approximation order L of the basis functions.

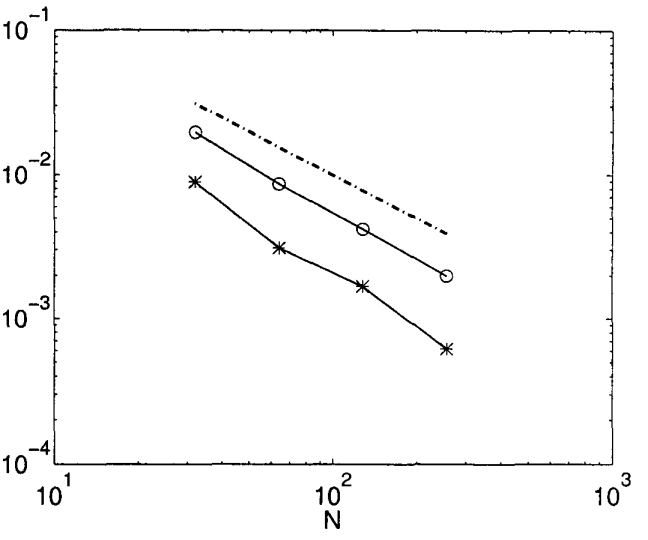

Figure 3: Approximation errors on voltage (circles) and current (stars) as functions of N_φ for the matched 1:4 exponential line with trapezoidal pulse excitation. The dash-dotted line corresponds to a slope N_φ^{-1}.

basis functions. As expected, we have a power law decay of the type N_φ^{-L}. Consequently, small errors can be obtained by using few high order basis functions.

We repeated the same analysis by using a 50% trapezoidal pulse voltage source with a rise time $\tau = 0.4$ s. This function has a singluarity in the first derivative. Therefore, the decay of the approximation error cannot be faster than N_φ^{-1} for any choice of basis functions. This is confirmed by Figure 3, which shows the behavior of the approximation error for voltage and current in the case of piecewise linear functions.

Nonparallel wires above a ground plane

This section will examine the crosstalk on a nonuniform line made of two wires above a ground plane, sketched below.

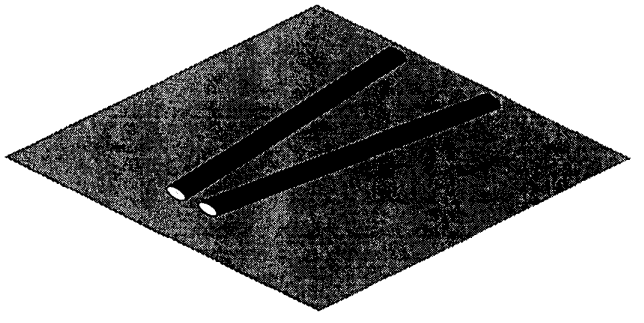

The two wires are supposed to be parallel to the ground plane, but their distance increases linearly along the length of the line. Lines of this type have been studied in [7, 2].

Let us consider two wires with radius $r = 1$ mm placed at $h = 3$ cm above a ground plane. Their separation is $D_0 = 5$ mm at $z = 0$ and $D_1 = 15$ mm at $z = 1$. The medium is supposed to be free space. Due to these particular conditions, the expressions for the per-unit-length inductance and capacitance matrices can be obtained with the wide-separation approximation [8]. Taking the ground plane as the reference conductor, we have the approximate expressions

$$L_{11} = L_{22} = \frac{\mu_0}{2\pi} \log\left(\frac{2h}{r}\right),$$

$$L_{12}(z) = L_{21}(z) = \frac{\mu_0}{4\pi} \log\left(1 + \frac{4h^2}{D^2(z)}\right),$$

where μ_0 indicates the permeability of free space and the distance along the line is

$$D(z) = D_0 + z(D_1 - D_0).$$

As the surrounding medium is homogeneous we can easily derive the per-unit-length capacitance matrix,

$$\mathbf{C}(z) = \varepsilon_0 \mu_0 \mathbf{L}^{-1}(z),$$

where ε_0 is the permettivity of free space.

We will apply a voltage source consisting of a 1 MHz , 50% duty cycle trapezoidal pulse train with raise and fall times equal to 20 ns to one of the two wires at the edge $z = 0$, and calculate the near end crosstalk on the other

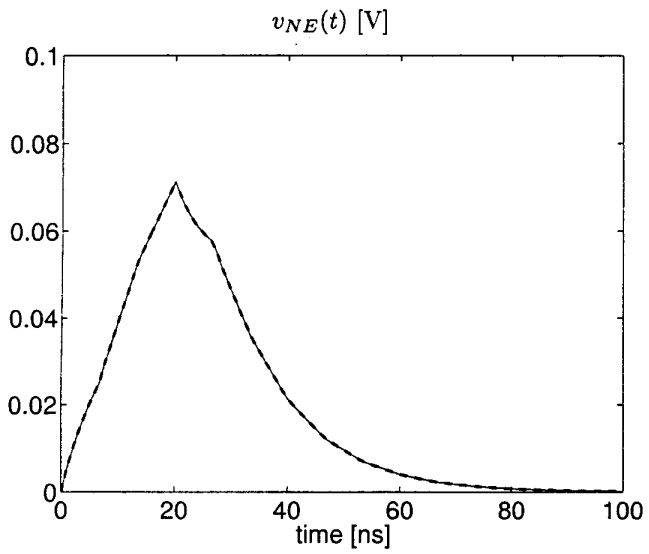

Figure 4: Near end crosstalk for the nonparallel wires above a ground plane. The thin continuous line represents the weak solution and the thick dashed line is the reference solution.

wire. Each conductor is terminated with a 50 Ω resistance connected to the reference.

As there is no closed form solution for lines of this type, we used an approximate method to obtain a reference solution for this problem. The standard approach is to divide the line into N_z uniform subsections and to perform the analysis in the frequency domain [8, 2]. Each subsection is analyzed separately by deriving its chain matrix, which can be evaluated in closed form. The chain matrix of the overall structure is then obtained by multiplying the chain matrices of each subsection of the line, and the solution for the voltages and currents at the line ends is found by incorporating the terminal conditions. Finally, inverse FFT is applied to get the time domain waveform. This method converges to the exact solution when N_z increases. Some numerical tests on the convergence have been conducted to obtain the minimum number of subdivisions that insures a good approximation for the nonuniformity of the line. A number of $N_z = 32$ subdivisions resulted beyond this limit and was used in the simulations.

Figure 4 shows the results of the simulations with our method ($N_\varphi = 65$) and with the approximate piecewise uniform solution. The number of points for the evaluation of the inverse FFT in the latter was set to 1024. The two curves are undistinguishable. We can conclude that the two methods give practically the same results.

CONCLUSIONS

A new time-domain scheme for the numerical solution of the Nonuniform Multiconductor Transmission Lines (NMTL) has been presented. The method is based on the spatial expansion of the solution, the external sources, and the per unit length matrices into some approximating functions. The projection of the NMTL equations through suitable test functions leads to a discrete system of ODE's that can be solved by an appropriate time integration scheme. The approximation order of the method depends on the particular choice of trial and test functions. Numerical tests show that small approximation errors can be obtained with few high order basis functions.

REFERENCES

[1] C. E. Baum, J. B. Nitsch, and R. J. Sturm, "Analytical Solution for Uniform and Nonuniform Multiconductor Transmission Lines with Sources", *The Review of Radio Science* 1993-96, URSI-Oxford University Press, 1996, NY.

[2] P. Besnier, and P. Degauque, "Electromagnetic Topology: Investigations of Nonuniform Transmission Line Networks", *IEEE Trans. Electromagn. Compat.*, vol. 37, 1995, 227-233.

[3] C. R. Burrows, "The exponential transmission line", *Bell System Tech. J.*, vol. 17, 1938, 555-573p.

[4] F. Chang, "Transient Simulation of Nonuniform Coupled Lossy Transmission Lines Characterized with Frequency-Dependent Parameters-Part I: Waveform Relaxation Analysis", *IEEE Trans. Circuits Syst. I*, vol. 39, 1992, 585-603.

[5] T. Dhaene, L. Martens, and D. De Zutter, "Transient Simulation of Arbitrary Nonuniform Interconnection Structures Characterized by Scattering Parameters", *IEEE Trans. Circuits Syst. I*, vol. 39, 1992, 928-937.

[6] IMSL, *IMSL MATH/LIBRARY User's Manual, Version 2.0*, 1991, IMSL, Houston.

[7] J. Nitsch, C. E. Baum , "Splitting of degenerate natural frequencies in coupled two-conductor lines by distance variation", Interaction Notes, Note 477, July 1989.

[8] C. R. Paul, *Analysis of Multiconductor Transmission Lines*, John Wiley and Sons, NY, 1994.

[9] V. K. Tripathi, N. Orhanovic, "Time-Domain Characterization and Analysis of Dispersive Dissipative Interconnects", *IEEE Trans. Circuits Syst. I*, vol. 39, 1992, 938-945.